J Mater Sci (2010) 45:969–978
DOI 10.1007/s10853-009-4027-1

Dry sliding wear of eutectic Al–Si

I. Baker · Y. Sun · F. E. Kennedy · P. R. Munroe

Received: 4 August 2009 / Accepted: 7 November 2009 / Published online: 24 November 2009

Abstract The wear of as-cast eutectic Al–Si was studied using pin-on-disk tribotests in two different environments, air and dry argon. The counterface in all tests was yttria-stabilized zirconia. It was found that wear of the Al–Si was reduced by about 60% by the removal of oxygen from the test environment. The zirconia counterfaces showed measurable wear after tests performed in air, while there was very little wear of the zirconia for tests conducted under argon. The near-surface regions of the Al–Si pins were examined using a transmission electron microscope (TEM), using specimens produced by focussed ion beam milling. The specimens that had been worn in air were characterized by a near-surface mechanically mixed layer containing a considerable amount of both aluminum oxide and zirconium oxide—the aluminum oxide particles had evidently acted as abrasive agents to remove material from the zirconia counterface. In contrast, TEM analysis of the Al–Si tested in argon showed little zirconium oxide in the near-surface regions.

Introduction

Aluminum–silicon alloys are of considerable and growing interest for use in automobile engines and in other applications in which they may slide against other materials. The interest in these materials is driven by their light weight, good castability, and relatively high strength/weight ratio, but for tribological applications an even more important characteristic is their wear resistance.

It has been known for many years that the sliding wear of Al–Si alloys generally falls in the mild wear regime at low normal loads and in the severe wear regime at high loads [1, 2]. The severe wear regime is characterized by high wear rates and often by transfer of aluminum material to the counterface. There is considerable plastic deformation of the Al–Si material near the contact surface and significant fragmentation, compaction, and mechanical mixing within the heavily deformed near-surface layers; these near-surface layers have been called "mechanically mixed layers" [3, 4] or "tribolayers" [5]. Wear particles have been reported to originate through crack initiation and propagation within the near-surface layers [2, 5, 6]. The mild wear regime has wear rates that may be an order of magnitude lower than severe wear rates and generally has oxidized layers on the sliding surface that are at least partially responsible for the lower wear in the mild regime [7]. The mechanically mixed layer beneath the surface has also been found to contain fine oxide particles, particularly at high loads and high sliding speeds [4, 5]. The transition between mild and severe regimes has been related to the transition between oxidation wear, in which the oxidation products are somewhat protective, and metallic wear, in which defects in the mechanically mixed layer result in the generation of more and larger wear particles [1, 7]. The oxidative wear mechanism has been studied in detail by several authors, and it has been suggested that the oxidation occurs primarily within the real area of sliding contact owing to frictional heating of the contacting materials

I. Baker (✉) · Y. Sun · F. E. Kennedy
Thayer School of Engineering, Dartmouth College, Hanover, NH 03755-8000, USA
e-mail: ian.baker@dartmouth.edu

P. R. Munroe
Electron Microscope Unit, University of New South Wales, Sydney, NSW 2052, Australia

[8, 9]. Although the oxide, generally Al_2O_3, is often protective and results in lower wear rates [10], the oxide particles can also be detrimental, as will be shown below.

Recent studies have shown that lubrication of the sliding contact can produce another wear regime, ultra-mild wear, for some *hypereutectic* and *eutectic* Al–Si alloys when sliding at relatively low loads in boundary lubricated conditions [11, 12]. Wear of the Al–Si alloys in such lubricated sliding cases is reduced by an oil residue layer on the sliding surfaces, resulting in a wear rate that can be several orders of magnitude lower than for unlubricated mild wear [13].

There has been considerable research in recent years into the wear mechanisms of Al–Si alloys and into measures that can be taken to increase the wear resistance. In addition to the very beneficial effects of lubrication, it has been found that some reduction in wear can also be brought about by changes in silicon content [1, 2, 14] or by alloying additions that affect the size, shape, and distribution of Al and Si grains [15, 16]. In general, however, it is felt that significant reductions in wear of Al–Si alloys can best be achieved by controlling the formation and stability of the mechanically mixed layer or of protective tribolayers [5].

In a recent study by Li et al. [5], it was found that the wear rate of an Al–Si alloy in dry sliding against a hardened 52100 steel was about 10 times lower when the test was conducted in an argon environment than when the test was conducted in air. They analyzed the mechanically mixed layers (or tribolayers) and found that the layers formed in air contained a large amount of oxide and were somewhat fragmented, whereas much less oxide was found in the layers after tests in argon and those layers were more compact [5]. There was also more transferred iron in the mechanically mixed layer after the tests in air, although the role of the iron was not completely clear. A similar effect of test environment was found in earlier studies of the wear of the ordered intermetallic alloy NiAl, which showed that wear increases as the amount of oxygen in the environment increases [17, 18]. In that work, the primary factor leading to increased wear in oxygen environments was determined to be the presence of abrasive third-body wear debris composed of oxides of nickel and aluminum. Thus, although oxidation can be beneficial in reducing wear under mild wear conditions, it can sometimes be detrimental and lead to a considerable increase in wear.

The objective of this study was to determine the influence of oxygen in the environment on the wear of *eutectic* Al–Si during dry sliding. In order to eliminate the possibly confounding effects of iron or iron oxide that may occur in tests of aluminum alloys against a steel counterface, the tests in this study were run with an inert zirconia disk sliding against Al–Si pins.

Experimental

A 125 mm long by 25 mm diameter ingot of aluminum–silicon of eutectic composition (Al–12.6 at.% Si) was arc melted and drop-cast under argon.

For metallography, the alloy was polished to a 1 μm surface finish using silicon carbide paper followed by alumina powder and etched using 20% nitric acid in methanol. Specimens were examined using backscattered electron (BE) imaging on a FEI XL-30 field emission gun scanning electron microscope (SEM) operated at 15 kV.

Transmission electron microscope (TEM) specimens of the as-cast alloy were prepared using a Fei Nova 200 Nanolab focussed ion beam microscope (FIB) using the lift-out method [19]. As a precursor to TEM specimen preparation, platinum was deposited in situ to protect the regions of interest from ion beam damage. Thinned samples were subject to ex-situ lift-out and examined in a Philips CM200 TEM operating at 200 kV to which an energy dispersive X-ray spectrometer (EDS) was interfaced. Elemental X-ray maps were collected with this instrument operating in STEM mode.

In order to characterize the material, two tensile tests were performed at an initial strain rate of 1×10^{-4} s^{-1} in air on cylindrical, dumbell-shaped tensile specimens (gauge length—9 mm; gauge diameter—3.8 mm; radius of curvature of shoulder—1.9 mm) machined from the as-cast alloy. The fracture surfaces were examined using secondary electron (SE) imaging on the XL-30 SEM operated at 15 kV. Microhardness tests of the flat, unworn surfaces of Al–Si pins were performed using a Leitz Miniload hardness tester with a 200 g testing load.

Pin-on-disk wear tests were performed against an yttria-stabilized zirconia counterface polished to a surface roughness of ~0.01–0.05 μm. The test device is described in detail in Johnson et al. [20]. The hot-isostatically pressed zirconia disk with zero porosity had been doped with yttria (Y_2O_3) to fully stabilize it. By varying the pin's sliding radius, approximately 10 tests could be accommodated on each side of the disk before resurfacing. Resurfacing was performed with a diamond-embedded grinding wheel to give a disk surface roughness (Ra) ranging from 0.01 to 0.05 μm.

The cylindrical pins were 9.5 mm diameter with a hemispherical tip; all pins were ground to shape and then polished to a mirror finish. Tests were carried out at room temperature (22–25 °C) in an environmental chamber either in air (30–45% relative humidity) or under flowing dry argon to minimize the possibility of oxidation contributing to the wear results. Three pins were tested in air and five pins were tested under argon. The pins were stationary and were held against the moving zirconia disk with a normal load of 23 N. The tests were run at a

constant sliding speed of 1 m s^{-1} for a total sliding distance of 1 km. A strain gage force transducer on the pin holder allowed continuous measurement of friction forces.

Mass measurements of the Al–Si pins before and after testing provided a total mass loss resulting from wear. At least five measurements were made of the pin mass in each condition and mean values were determined. The density of the Al–Si material, measured to be 2.654 g/cm^3, was used to convert mass loss into volumetric wear. Wear of the zirconia disk was measured after some tests using linear profilometry. Four radial traces were taken across the circular wear track on the disk at equally spaced (90°) intervals. Analysis of the traces enabled the mean depth and width of the wear track to be determined, and those values, along with the mean wear track radius, were used to determine volumetric wear of the zirconia disk.

Debris was collected during the wear tests by using adhesive tape wrapped around the outside of the zirconia disk. X-ray diffractometer traces were obtained from the debris using a Siemens D5000 operated at 40 KV, 30 mA producing CuK radiation and equipped with a Kevex solid state detector. Measurements were performed by step scanning 2θ from 10° to 120° with a 0.01° step size. A count time of 2 s per step was used, giving a total scan time of ~6 h.

The wear surfaces were examined using SE imaging on the XL-30 SEM operated at either 15 or 30 kV. Subsurface damage on the wear surface was investigated using both FIB microscopy and a TEM, as noted above. FIB cross-sections were prepared using a Fei xP200 FIB. Cross-sections into the wear surface were milled using a gallium ion beam, using beam currents of 6600 pA for the initial cuts and 1000 pA for the final cleaning mills. Images were recorded using ion beam induced secondary electrons. TEM specimen preparation was performed as described earlier.

Results and discussion

Figure 1 is an BE image of the as-cast microstructure, which consists of Al and Si grains. Figure 2a is a bright field TEM image of the as-cast microstructure. The microstructure consisted of fine Al grains, which contained numerous subgrains and Si grains. Figure 2b shows X-ray maps using Al, O, and Si K X-ray peaks from the region around the interface between the Si and Al grains in Fig. 2a. Relatively small amounts of Al_2O_3 were present at the interface, but alumina was not commonly found in regions away from the interface between Al and Si.

Figure 3 shows a stress–displacement curve for the as-cast alloy. The average yield strength and failure stress for the two tests were around 130 and 177 MPa, respectively.

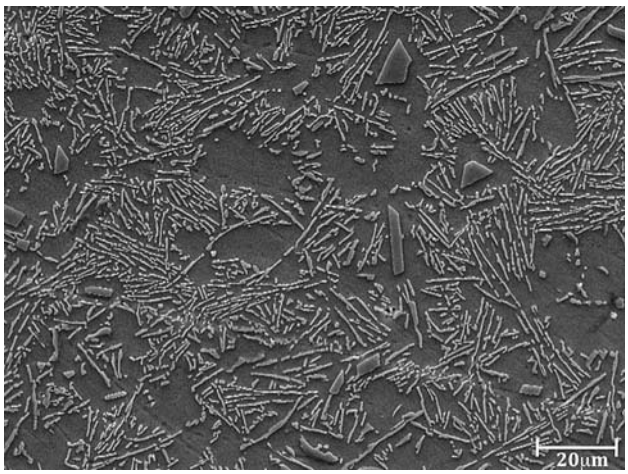

Fig. 1 Backscattered electron image of the as-cast microstructure after etching with concentrated sodium hydroxide/water solution

The elongation to failure was ~7% and the modulus of elasticity was approximately 70 GPa. Examination of the fracture surface in the SEM showed a ductile looking fracture mode, see Fig. 4. The aluminum seems to have flowed around the Si during deformation.

Microhardness tests were performed on the unworn Al–Si pin specimens, and it was found that the average hardness was 462 MPa, slightly more than three times the average yield strength, as expected for a ductile material. It might be noted that the hardness is somewhat higher than that of pure aluminum (250–450 MPa) [21], but much lower than that of pure silicon (8 GPa) [22].

The results of the wear tests are summarized in Fig. 5. The mean mass loss of Al–Si pins after 1 km of sliding in air (5.53 mg) was more than 2.5-times the mass loss from tests performed in argon (2.10 mg). These correspond to volumetric wear rates of 2.1 mm^3/km in air and 0.79 mm^3/km in argon. Analysis of the wear data showed that the difference between wear in air and wear in argon was statistically significant ($p < 0.05$). A significant difference between wear rate in air and wear rate in argon was also found in the study by Li et al. [5], but it might be noted that the wear in air was 2.5-times the wear in argon in these tests, but was 10-times greater than the wear in argon in the tests reported in [5]. The primary reason for this difference is probably the fact that Li et al. [5] studied a hypereutectic Al–Si alloy (A390) in contact with a hard steel (52100) counterface, whereas eutectic Al–Si was tested against zirconia in this study.

The measured friction force was somewhat variable during the tribotests, and decreased from a higher initial value to a lower steady state value in both test environments. The measured friction coefficient (steady state) was approximately 0.4 for tests conducted in air, but was a bit lower (about 0.35) for tests conducted in argon.

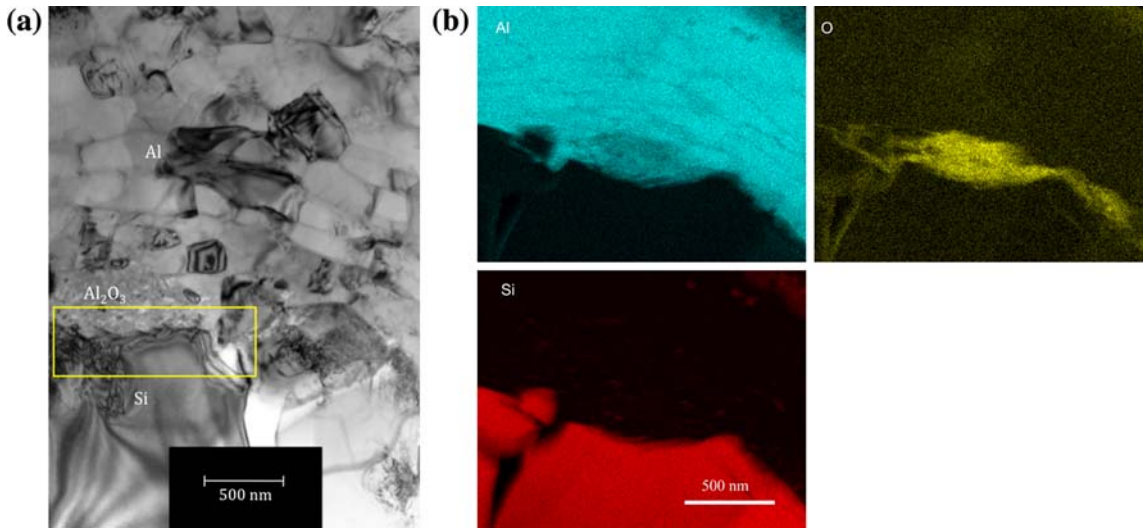

Fig. 2 **a** Bright field TEM image of the as-cast microstructure. The *yellow box* shows the region from which the X-ray maps were taken. **b** X-ray maps using Al, O, and Si peaks from the region around the interface between the Si and Al grains in **a**

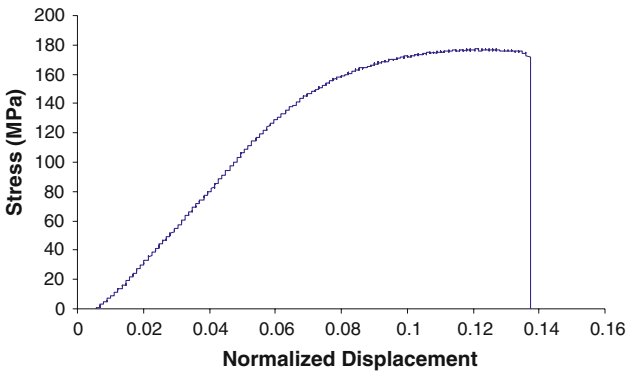

Fig. 3 Tensile stress–displacement curve for as-cast eutectic Al–Si

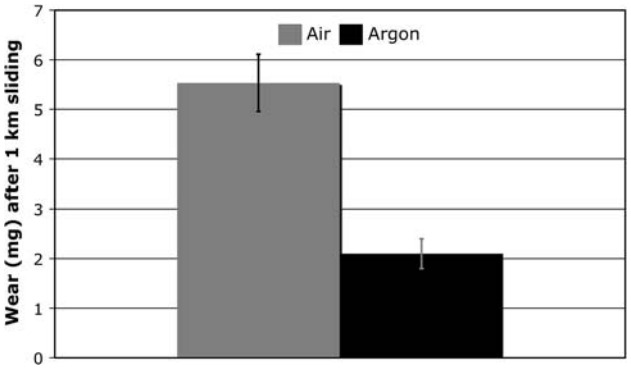

Fig. 5 Wear (mean value of mass loss) of Al–Si pins after 1-km sliding tests in air and in dry argon. Three tests were performed in each environment. Error bars signify standard deviation

The wear tracks on the zirconia disk showed significant wear after tests conducted in air, but very little wear after tests carried out in argon. The mean depth of the wear track on the zirconia disk after a 1 km sliding test in air was 7.37 μm, and the corresponding mean volumetric wear was 7.9 mm^3. In contrast, after wear tests conducted in argon the zirconia disk showed essentially no wear, and in fact the surface of the wear track was actually built up (by an average of about 0.34 μm in a typical test) due to the presence of a transferred film of aluminum on the wear track. Less transferred aluminum was found on the surface

Fig. 4 SE image of the fracture surface of tensile-tested as-cast eutectic Al–Si

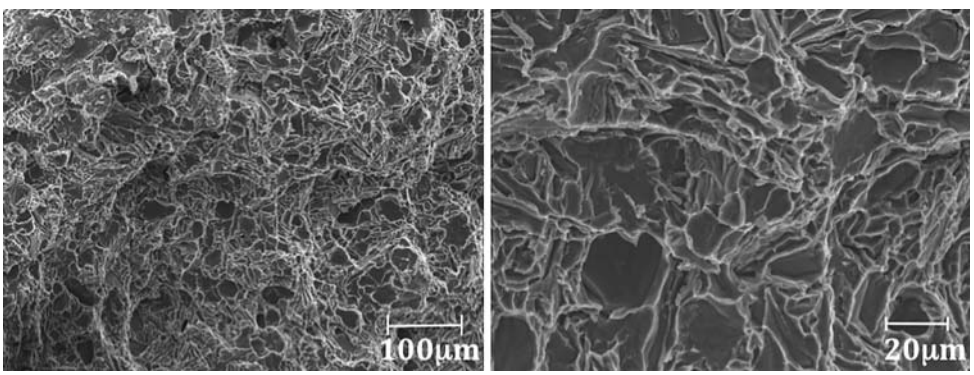

of the wear track after tests performed in air, presumably because the transfer film was worn away soon after it formed. Comparison of the volumetric wear rate measured for the Al–Si pins with the wear volume of the zirconia disk shows that for the tests conducted in argon a large percentage (nearly half) of the material worn from the Al–Si pins ended up as transfer film on the zirconia disk. On the other hand, with tests performed in air the volumetric wear of the zirconia was even greater than that of the Al–Si pins. That result is rather surprising, since zirconia is much harder and more wear resistant than aluminum–silicon alloys. The explanation is that the zirconia must have been worn or abraded during the tests. Although it is known that a material can be self-abraded (by particles of the same material) or even to some extent by materials with a lower hardness, in most cases abrasion is caused by contact with asperities or particles a harder material [21]. In this case, the abrasion of zirconia must have been carried out by alumina that resulted from oxidation of the aluminum matrix as a consequence of frictional heating. Alumina is generally harder (1500–2100 HV) than zirconia (1050–1300 HV) [21, 23], so abrasion of zirconia by the harder alumina is quite possible. Abrasion probably took place by a combination of two-body abrasion, by alumina particles embedded in and protruding from the Al–Si surface, and three-body abrasion, by alumina particles (and to some extent zirconia particles) that had been removed from the contacting surfaces and were tumbling in the space between the surfaces. Two-body abrasion is more effective than three-body abrasion in removing material (such as zirconia) from a surface [21], but both wear mechanisms appear to have been at play here.

An approximate analysis of the contact temperatures present at the Al–Si sliding interface in the wear tests resulting from frictional heating was performed. The calculations are included in "Appendix". It was found that the contact temperatures within the assumed Hertzian contact area on the Al–Si pin surface could easily have reached over 225 °C, a value that is sufficient to cause oxidation of aluminum [8]. Localized "flash" temperatures may have been significantly higher in concentrated asperity contacts. Thus, while the presence of water vapor during the oxidation process could have produced aluminum hydroxide, the fact that aluminum hydroxide decomposes above 180 °C makes its presence in debris, rather than aluminum oxide, unlikely.

Figure 6 shows an X-ray diffraction pattern of the debris collected from a wear test performed in air. Most of the clearly identifiable debris is zirconia, with a minority component of aluminum. The large amount of zirconia debris is consistent with the finding of considerable volumetric wear of the zirconia disk, as discussed above. Silicon was not detected, presumably because little was

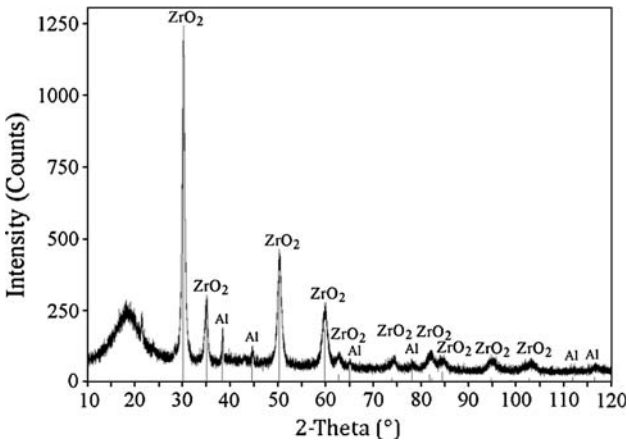

Fig. 6 X-ray diffraction pattern from debris collected from a wear test performed in air. The peak just below 20° is from the adhesive tape used to collect the powder

present. Although alumina is not observed in the pattern shown in Fig. 6, small amounts of alumina were found elsewhere in the collected debris. There was also a broad amorphous peak at $2\theta = 17°$ from the adhesive on the tape used to collect the debris. Note that it was not possible to perform a similar analysis for the tests conducted under argon due to the much smaller quantity of debris.

Examination of the worn surface of pins tested in air showed not only wear tracks, but also that material had been pulled out of the surface, see Fig. 7. This observation is consistent with the finding of aluminum in the X-ray diffraction patterns of the wear debris.

TEM specimens were removed from the pins using FIB machining. Figure 8 shows two examples of pits formed using the FIB, from which TEM specimens were taken.

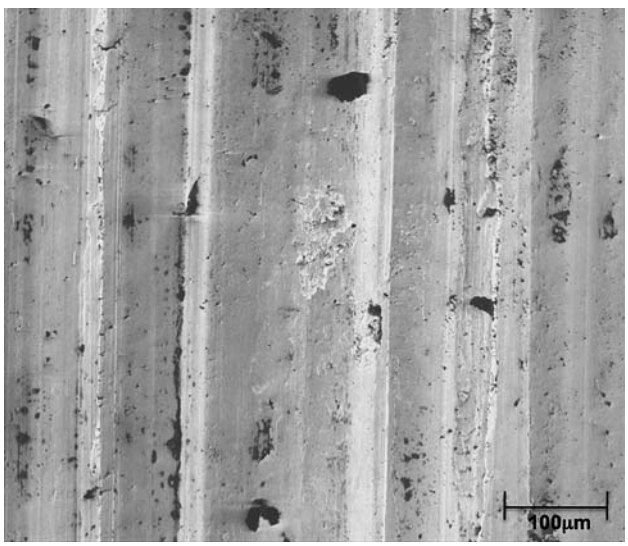

Fig. 7 Wear track on surface of Al–Si pin tested in air. Note the holes where material has been pulled out of the surface

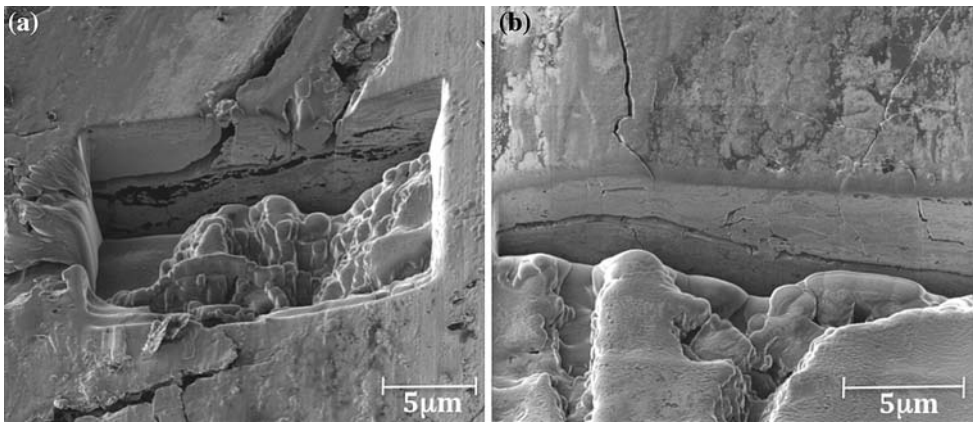

Fig. 8 SE image from pits produced using the FIB showing **a** an elongated layer of Si with a crack running above it, **b** from an area with few Si particles but with many subsurface cracks. From a specimen wear-tested in air

Figure 8a shows an elongated layer of Si with a crack running above it, while Fig. 8b shows an area with few Si particles, but with many subsurface cracks. In general, there was substantial subsurface cracking associated with the wear tracks although not all FIB'ed cross-sections showed subsurface cracking. The cracks only seem to penetrate about a micron into the surface and, broadly, do not appear to be associated with any specific microstructural features.

Figure 9 shows a bright field TEM image of the material close to the worn surface of the pin tested in air, and

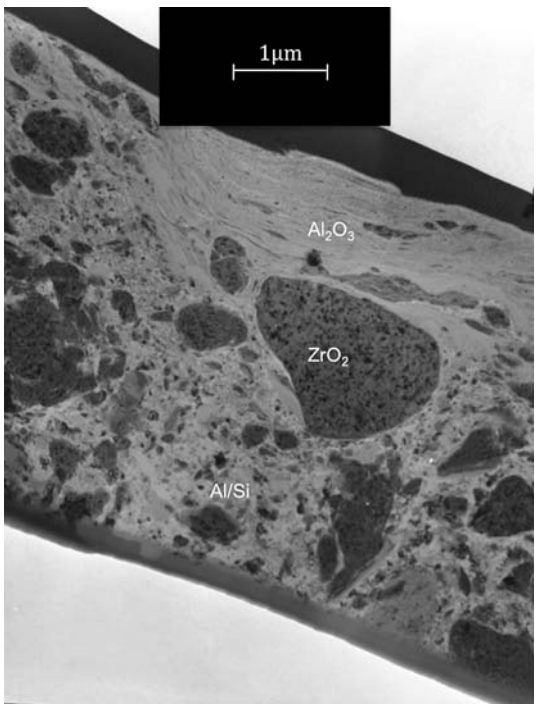

Fig. 9 Bright field TEM image of subsurface region in wear pin tested in air. The wear surface is at top. The Pt strip was deposited in the FIB to protect the surface while machining with the FIB. The region labeled Al/Si consists of fine-grained aluminium with fine particles of silicon. The *gray regions* with dark speckles, such as the one labeled, are zirconia

Fig. 10 shows X-ray elemental maps corresponding to the area in Fig. 9. An interesting feature is the incorporation of zirconia well below the worn surface of the pin. Thus, the particles worn from the zirconia disk had evidently been pulverized and mixed into the mechanically mixed layer that comprised the top few microns of the Al–Si pin. The outermost wear surface is alumina.

Figure 11 is an SEM image of a wear track on the surface of an Al–Si pin tested under argon. In contrast to the specimens tested in air, smearing of the surface occurred, and the pits where material had been pulled out of the surface for tests performed in air were not evident.

Figure 12 shows a cross-section produced by FIB machining from the wear track of the pin tested under argon. In the wall of the section, Si is the dark phase, alumina is the light phase, and the mid-gray colored matrix is the aluminum. Note the lack of subsurface cracking in the pin tested under argon, which is in sharp contrast to the tests performed in air.

Figure 13 shows a TEM image of the near-surface region of a specimen wear-tested under argon showing considerable mixing of phases. Unlike the tests performed in air, there are no zirconia particles in the subsurface region (compare to Fig. 9). However, there is considerable mixing in the layer and the subsurface structure is clearly different to the as-cast structure shown in Figs. 1 and 2. Figure 14 shows X-ray elemental maps for Al, Si, and O (no Zr was found so a Zr map was not produced) and a corresponding STEM image. Again the considerable mixing that has occurred is evident, with substantial amounts of aluminum oxide incorporated into the subsurface layers. Electron diffraction patterns from the subsurface regions of the pin tested in argon showed rings corresponding to aluminum, silicon and alumina only, consistent with the X-ray maps of Fig. 14, which show that no zirconia was present.

Based on all of the above results, the wear process of the eutectic Al–Si material against zirconia in argon appears to be very much dependent on the environment in which the

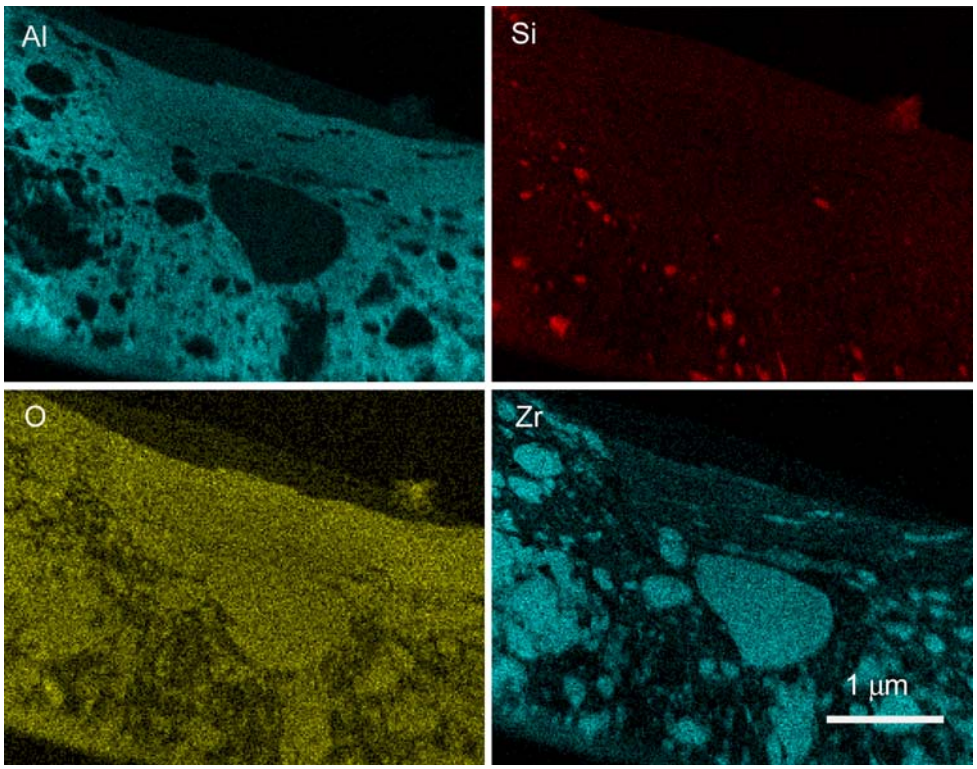

Fig. 10 X-ray maps for Al, Si, O, and Zr from the region shown in Fig. 9

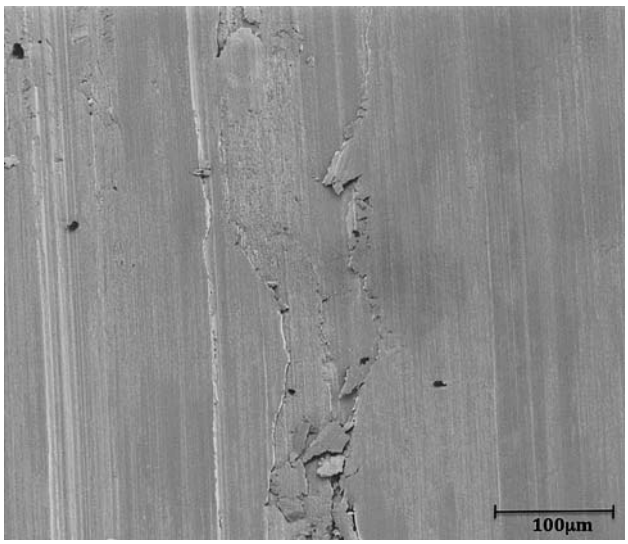

Fig. 11 SE image of a wear track on surface of Al–Si pin tested under argon. Note the smearing on the surface and the lack of pitting

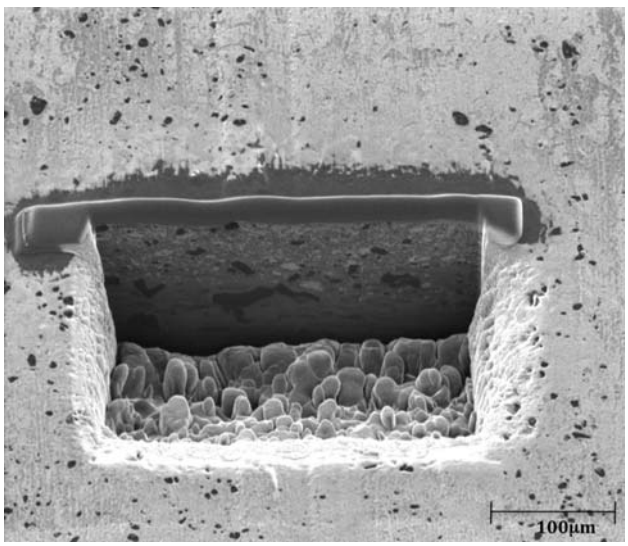

Fig. 12 SE image from pit in specimen wear-tested under argon from which TEM specimen was removed using a FIB. Si is the *dark phase*, alumina is the *light phase* and the *mid-gray colored* matrix is the aluminium. Note the lack of subsurface cracking subsurface cracking

tests are carried out. In an oxygen-free environment, such as dry argon, wear of the Al–Si takes place by near-surface deformation and damage accumulation, with wear particles detaching from the deformed layer and transferring to the counterface. This is similar to the mechanisms described by other authors, e.g., [7] for relatively mild wear of Al–Si against other counterfaces. In an oxygen-containing environment, however, the wear process is abetted by oxidation of the Al–Si material resulting from frictional heating, resulting in the creation of hard aluminum oxide particles. Some of the alumina particles remain on the Al–Si pin surface, where they act as abrasive asperities (two-body abrasion), while others are pulled out of the Al–Si surface and become abrasive third bodies. The alumina particles are hard enough to abrade the zirconia counterface. The

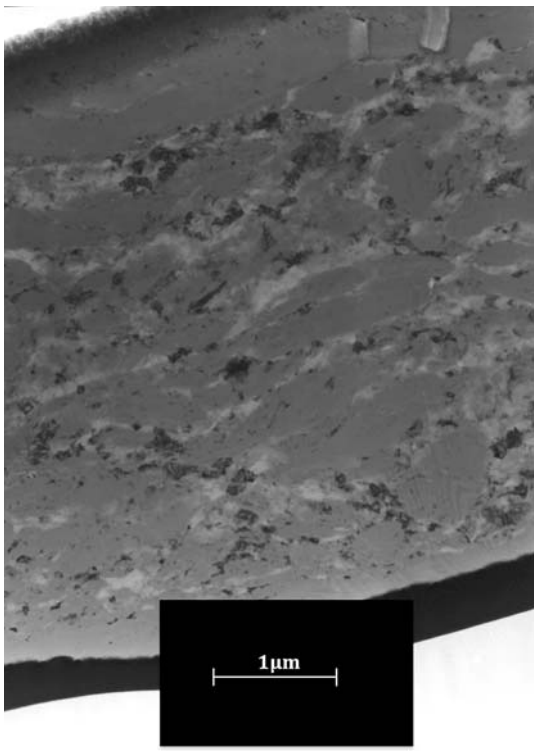

Fig. 13 TEM image of subsurface region in wear pin tested under argon showing mixed aluminium, alumina, and silicon

resulting zirconium oxide particles can become pulverized and mixed into the mechanically mixed layer on the surface of the Al–Si material. Damage to the mechanically mixed layer, particularly subsurface cracking, can result in the production of wear particles from the Al–Si material. The detrimental effect of oxidation on the wear of eutectic Al–Si in air at reasonably high sliding speeds that was clearly demonstrated in this work is consistent with results found in earlier studies of wear of NiAl [17] and hypereutectic Al–Si [5] in environments containing oxygen.

Summary and conclusions

The wear of as-cast eutectic Al–Si against an yttria-stabilized zirconia counterface was studied using pin-on-disk tribotests in two different environments, air and dry argon. The wear rate of the pins tested in air was more than twice that of those tested under argon. Similarly, the zirconia counterface showed much less wear for tests conducted under argon. TEM examination of the near-surface region of the pins that had been worn in air showed mechanically mixed regions with considerable amounts of both aluminum oxide and zirconium oxide—the aluminum oxide particles had evidently acted as abrasive particles to

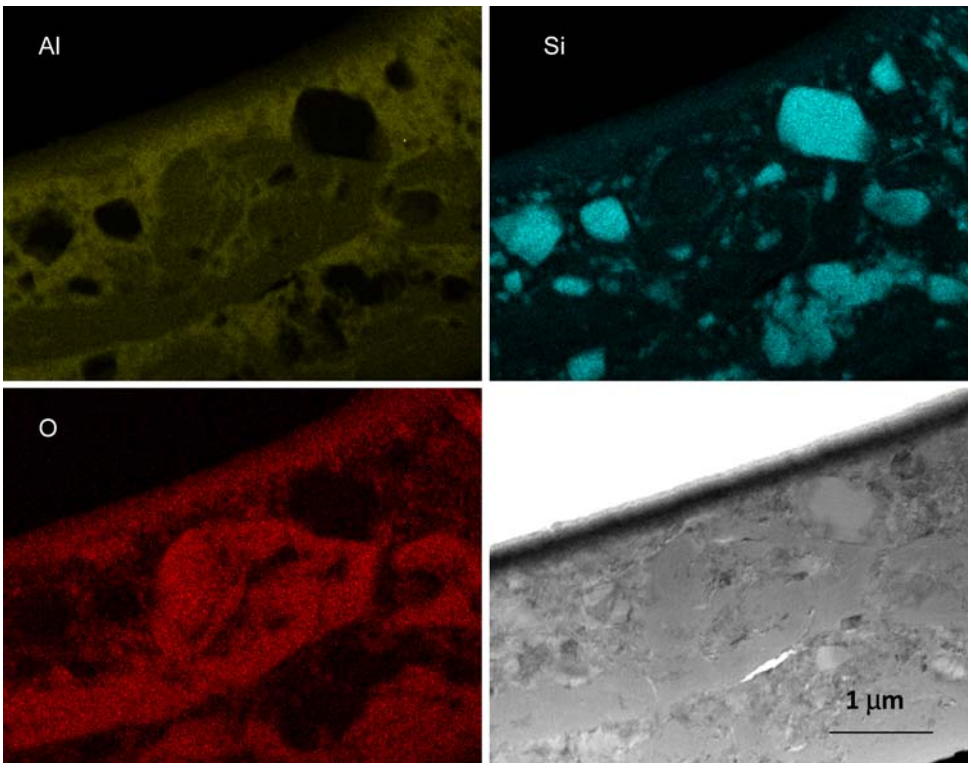

Fig. 14 X-ray maps for Al, Si, and O (A Zr map is not shown since no Zr was found) and corresponding STEM image of subsurface region in wear pin tested under argon

remove material from the zirconia counterface. In contrast, the pins tested in argon showed little zirconium oxide in the near-surface regions.

Acknowledgements This research was supported by the U.S. National Science Foundation (NSF) grant CMMI-0651642. The views and conclusions contained herein are those of the authors and should not be interpreted as necessarily representing official policies, either expressed or implied, of the NSF or the U.S. Government. We would like to acknowledge the help of Dr. Charles Daghlian and Michael Gwaze.

Appendix: Calculation of contact area and contact temperature

Contact of stationary Al–Si pin with moving Zirconia disk

Operating conditions:

Normal load $w = 23$ N	Sliding velocity $V = 1$ m/s
Friction coefficient (measured) $\mu = 0.4$	Pin radius $R_{\text{pin}} = 4.75$ mm

Material properties (* measured, remainder from [22])

	Al–Si (material 2)	Zirconia (material 1)
H Hardness (GPa)	0.462*	14
E Modulus of Elasticity (GPa)	70*	290
ρ Density (kg/m^3)	2654*	6100
ν Poisson's ratio	0.33	0.24
K Thermal Conductivity (W/m K)	140	1.8
C Specific heat (Nm/kg K)		630

Contact Geometry (assuming Hertzian contact [21])

$$\text{Radius of contact circle} \quad b = \left(\frac{3wr}{4E'}\right)^{1/3} \tag{1}$$

$$\text{Effective modulus} \quad E' = \left[\frac{1-\nu_1^2}{E_1} + \frac{1-\nu_2^2}{E_2}\right]^{-1} = 62.5\,\text{GPa} \tag{2}$$

$$\text{Effective radius} \quad r = \left[\frac{1}{R_{\text{pin}}} + \frac{1}{R_{\text{disk}}}\right]^{-1} = 0.00475\,\text{m} \tag{3}$$

Using 2 and 3 and operating parameters in 1 find the contact radius

$$b = 109\mu\text{m} \tag{4}$$

Contact Temperature rise (following methodology of [24])

Assume stationary Al–Si pin (material 2) and moving flat Zirconia disk (material 2)

$$\Delta T_{\max} = \frac{2.733\bar{q}_{\text{total}} b}{2.32K_2 + 1.178K_1\sqrt{\pi(1.234 + Pe_1)}} \tag{5}$$

$$\text{where Peclet number } Pe_1 = \frac{Vb\rho_1 C_1}{2K_1} = 116 \tag{6}$$

and

$$\text{average total heat flux } \bar{q}_{\text{total}} = \mu\left(\frac{w}{\pi b^2}\right)V = 246 \times 10^6\,\text{W/m}^2 \tag{7}$$

Using 5, 6, 7, and the material properties (above) in 5, find the peak contact temperature rise (above room temperature) $\Delta T_{\max} = 200$ °C.

This is the temperature rise due to frictional heating for the Hertzian contact. Given that the tests were conducted at room temperature (about 25 °C), the surface temperature at the center of the Hertzian contact area was thus at least $T_{\max} = 225$ °C.

It should be noted that the temperature analysis outlined above gives a relatively conservative estimate of the contact temperature at the interface between the hemispherically shaped Al–Si pin and the flat zirconia disk, since a single Hertzian (elastic) contact was assumed. The contacting material within the Hertzian contact region on the stationary Al–Si pin would remain at an elevated temperature for a substantial period of time, allowing plenty of time for oxidation to occur, even at 225 °C [8]. In the actual contact, it is probable that at any instant the real area of contact within the Hertzian region consisted of a finite number of concentrated asperity-level contacts. The peak contact temperature rise could be considerably higher at localized asperity contacts, but these would be of shorter duration (flash temperature rise).

References

1. Shivanath R, Sengupta PK, Eyre TS (1977) Wear of aluminium-silicon alloys. Wear of materials 1977. ASME, New York
2. Sarkar AD, Clarke J (1980) Wear 61:157
3. Rigney DA (2000) Wear 245:1
4. Li XY, Tandon KN (2000) Wear 245:148
5. Li J, Elmadagli M, Gertsman VY, Lo J, Alpas AT (2006) Mater Sci Eng A421:317
6. Akarca SS, Altenhof WJ, Alpas AT (2007) Tribol Int 40:735
7. Elmadagli M, Alpas AT (2006) Wear 261:367
8. Razavizadeh K, Eyre TS (1982) Wear 79:325

9. Quinn TFJ (1983) Tribol Int 16:257
10. Basavakumar KG, Mukunda PG, Chakraborty M (2007) J Mater Sci 42:7882. doi:10.1007/s10853-007-1633-7
11. Chen M, Perry T, Alpas AT (2007) Wear 263:552
12. Chen M, Alpas AT (2008) Wear 265:186
13. Chen M, Meng-Burany X, Perry TA, Alpas AT (2008) Acta Mater 56:5605
14. Xu CL, Yang YF, Wang HY, Jiang QC (2007) J Mater Sci 42:6331. doi:10.1007/s10853-006-1189-y
15. Dwivedi DK (2006) Mater Des 27:610
16. Basavakumar KG, Mukunda PG, Chakraborty M (2007) J Mater Proc Tech 186:236
17. Kennedy FE, George M, Baker I, Johnson BJ, Chang N (1996) Influence of composition and environment on wear of NiAl and Ni–Fe–Al. In: Proceedings of the international tribology conference, Yokohama 1995. Japanese Society of Tribologists I, pp 337–342
18. Munroe PR, Baker I, George M, Kennedy FE (2002) Mater Sci Eng A325:1
19. Giannuzzi LA, Stevie FA (1999) Micron 30:97
20. Johnson BJ, Kennedy FE, Baker I (1996) Wear 192:241
21. Hutchings IM (1992) Tribology, friction and wear of engineering materials. CRC Press, Boca Raton, FL
22. Bhushan B, Gupta BK (1991) Handbook of tribology. McGraw-Hill, New York
23. Murray SF (1997) Properties of advanced ceramics. Tribology data handbook. CRC Press, Boca Raton, FL
24. Kennedy FE (2001) In: Bhushan B (ed) CRC handbook of modern tribology. CRC Press, Boca Raton, FL, p 235